PCCP

ROYAL SOCIETY OF CHEMISTRY

PERSPECTIVE

View Article Online
View Journal | View Issue

Cite this: *Phys. Chem. Chem. Phys.*, 2022, **24**, 15173

Dipolar spin–spin coupling as an auxiliary tool for the structure determination of small isolated molecules

Luca Bizzocchi, *[a] Silvia Alessandrini, *[ab] Mattia Melosso *[ac] and Cristina Puzzarini *[a]

Received 7th March 2022,
Accepted 16th May 2022

DOI: 10.1039/d2cp01124g

rsc.li/pccp

The "gold standard" for obtaining accurate equilibrium structures is the so-called semi-experimental (SE) approach, which exploits the structural information contained in rotational constants. Within the SE approach, ground-state rotational constants—accurately obtained from high-resolution spectroscopic studies—are computationally corrected in order to remove vibrational effects. The resulting SE equilibrium rotational constants for a significant set of isotopic species allow for retrieving a unique set of equilibrium bond lengths and angles for the molecule under consideration. However, in some cases, the lack of isotopic substitution hampers or even prevents a rigorous and complete structure determination. In this perspective, we introduce the use of dipolar spin–spin coupling constants as an additional source of structural information in support of the standard SE approach. As a proof-of-concept, we tested this new strategy on some prototypical species, such as water, ammonia, phosphine, and their fluorinated counterparts. Our results indicate that—even when the molecular structure can be obtained from a large set of isotopic rotational constants—the use of dipolar spin–spin coupling constants guarantees a better accuracy and reduces the correlations among the geometrical parameters. Moreover, we point out that our approach offers the possibility to fully derive the molecular structure of PF_3, a species for which any isotopic substitution is not possible.

1 Introduction

The knowledge of the structural properties and dynamic behavior of molecules is at the heart of a deep understanding of their stability, spectroscopy, and reactivity. The accurate determination of molecular structures is thus one of the principal aims in many areas of physical chemistry and chemical physics, which—in the last few decades—has involved the efforts of experimentalists and theoreticians.[1,2] In particular, for all spectroscopies, there is a strong relationship between the experimental outcome and the underlying electronic structure of the system under consideration (see, for example, ref. 3–7). In this respect, a great advantage of molecular spectroscopy is the capability of probing molecular properties in a non-invasive manner. In the gas phase, rotational spectroscopy is the technique of choice to derive accurate structural information because of the strong dependence of the rotational constants on the molecular geometry.[5,8–12] Unfortunately, it is seldom straightforward to retrieve the molecular structure from the experimental information. Indeed, for a given molecule, there are at most three rotational constants, with the structural parameters being up to $3N - 6$ (where N is the number of atoms). The way-out is to resort to different isotopic species of the same molecule in order to increase the number of data. Different isotopologues of a given molecule share the same equilibrium structure (r_e), *i.e.* the minimum geometry on the Born–Oppenheimer potential energy surface but not the vibrationally averaged structure which depends on the atomic masses. This is the limitation hampering the vibrationally averaged r_0[8] structure that is obtained from the direct analysis of the vibrational ground-state rotational constants for different isotopologues, without any explicit consideration of vibrational effects.[1,2] As a consequence, vibrationally averaged structures depend on the set of isotopic species considered.[1,2] To avoid these limitations, one has to resort to r_e.

From a pure experimental point of view, for small molecules, it might be feasible to derive experimental vibrational contributions that can be used to correct the ground-state rotational constants. The equilibrium rotational constants then obtained for different isotopic species can be used for the determination

[a] *Dipartimento di Chimica "Giacomo Ciamician", Università di Bologna, via F. Selmi 2, 40126 Bologna, Italy. E-mail: luca.bizzocchi@unibo.it, cristina.puzzarini@unibo.it*
[b] *Scuola Normale Superiore, Piazza dei Cavalieri 7, 56126 Pisa, Italy. E-mail: silvia.alessandrini@sns.it*
[c] *Scuola Superiore Meridionale, Università di Napoli Federico II, Largo San Marcellino 10, 80138 Naples, Italy. E-mail: mattia.melosso@unina.it*

of the equilibrium structure. However, such a procedure becomes unpractical already for medium-sized molecular systems. This difficulty can be efficiently tackled using the so-called semi-experimental (SE) approach.[2,9–11] Within this framework, quantum-chemical calculations are employed to recover vibrational effects. For different isotopologues, computed vibrational corrections are combined with the corresponding experimental ground-state rotational constants to obtain the so-called SE equilibrium rotational constants and, from them, the SE equilibrium structure. This method proved to be powerful and allowed the derivation of the accurate equilibrium structures of small- to medium-sized molecules and non-covalent molecular complexes,[2,5,10–17] thus superseding the previously used Kraitchman's substitution method (the r_s structure).[18] Since r_s structures do not explicitly and rigorously treat the vibrational contributions, they might lead to inaccurate and biased results.[5]

However, the SE approach has some limitations, since a balanced fit is obtained only with a large set of experimental data including several isotopic substitutions. Ideally, one should have at least one isotopic substitution for each nucleus of the system under consideration.[2] This might be unpractical from an experimental point of view, but, in some cases, it can be simply impossible because of the lack of different stable isotopes for a given atom. This is the case, for example, for fluorine and phosphorous.

Interestingly, there are other spectroscopic parameters than the rotational constants that directly depend on the molecular geometry. This is the case of the dipolar spin–spin coupling constants, which describe the interaction of two nuclear magnetic moments in a molecule. In nuclear magnetic resonance (NMR), in the spectroscopic investigation of non-isotropic media, dipolar coupling interactions are responsible for the signal splitting and represent the dominant coupling mechanism.[19] In rotational spectroscopy, dipolar couplings are, in addition to spin-rotation interactions and nuclear quadrupole couplings, responsible for the hyperfine structure of the spectra.[5,8] The experimentally determined dipolar spin–spin coupling constants can be used to obtain the structural information even in those cases where isotopic substitutions are not feasible.[5] More generally, they can enrich the set of experimental data to be used in the SE approach.

This perspective inspects the use of dipolar spin–spin coupling constants in support of the SE structure determination. In particular, we explore their role when the isotopic substitution is limited or not feasible. For this purpose, we have selected three light hydrides and their fully fluorinated counterparts: (i) H_2O and OF_2, (ii) NH_3 and NF_3 and, (iii) PH_3 and PF_3. These have been chosen because they range from systems for which a large number of data are available with great precision, such as NH_3 and H_2O, to systems for which isotopic substitution is limited (OF_2 and NF_3) or not possible at all (such as PF_3). In the following, all relevant theoretical details of the form of the dipolar spin–spin coupling tensor are provided. Then, computational details and the methodology for the derivation of structural parameters are given. Subsequently, the results are collected and discussed.

2 Theoretical details

The dipolar interaction between the I_L and I_M nuclear magnetic moments is described by the following Hamiltonian

$$H_{\mathrm{dip}}^{\mathrm{LM}} = \mathbf{I}_{\mathrm{L}} \cdot \mathbf{D}^{\mathrm{LM}} \cdot \mathbf{I}_{\mathrm{M}}, \tag{1}$$

where $\mathbf{D}^{\mathrm{LM}}$ is the dipolar spin–spin coupling tensor, whose components in SI units are given by[5,8,19]

$$D_{\alpha\beta}^{\mathrm{LM}} = -\frac{g_{\mathrm{L}} g_{\mathrm{M}} \mu_N^2}{4\pi\varepsilon_0 c^2} \frac{3(\mathbf{R}_{\mathrm{LM}})_\alpha (\mathbf{R}_{\mathrm{LM}})_\beta - \delta_{\alpha\beta} \mathbf{R}_{\mathrm{LM}}^2}{R_{\mathrm{LM}}^5}, \tag{2}$$

From left to right: Cristina Puzzarini, Luca Bizzocchi, Silvia Alessandrini and Mattia Melosso

Four members of the ROT&Comp lab. From left to right: Cristina Puzzarini is a Professor of Physical Chemistry at the University of Bologna and Head of the ROT&Comp lab at the Department of Chemistry "Giacomo Ciamician"; her research activity spans from computational chemistry and spectroscopy to experimental rotational spectroscopy; her main research interest is astrochemistry, focusing on spectroscopic studies in support of astronomical observations and investigation of interstellar chemistry. Luca Bizzocchi received his PhD in Chemistry at the University of Bologna in 2002; he was a post-doctoral fellow in Bologna, Lisbon, and at the Max-Planck Institute for Extraterrestrial Physics, Garching; since 2021, he has a tenure-track professorship at the Department of Chemistry "Giacomo Ciamician"; his interests are in molecular physics and astrochemistry, with a particular focus on high-resolution molecular spectroscopy and millimetre-wave astronomy. Silvia Alessandrini is a young researcher in computational chemistry, who received her PhD cum laude in May 2022; her scientific interest involves the development and validation of accurate computational approaches for the modeling of gas-phase chemistry, to be exploited in support of experimental rotational spectroscopy and in astrochemistry. Mattia Melosso received his PhD in Chemistry at the University of Bologna in 2020; currently, he is a post-doc fellow at Scuola Superiore Meridionale in the area of Molecular Science for Earth and Space; his research interests are rotational and ro-vibrational spectroscopy and the discovery of new interstellar molecules.

where $\mathbf{R}_{LM}$ denotes the vector from nucleus L to M, g_L and g_M are the corresponding nuclear g-factors, ε_0 is the vacuum permittivity, c is the speed of light, and $\delta_{\alpha\beta}$ is Kronecker's delta with $\alpha,\beta = x, y, z$, cyclically. From eqn (2), it appears clear that the dipolar spin–spin coupling tensor is completely determined by the molecular geometry.

The tensor $\mathbf{D}$ is symmetric and traceless by definition and it is customary to express its diagonal elements (for a prolate-type rotor) as D_{zz} and D_{xx}–D_{yy}. For linear molecules, these reduce to one independent component due to the cylindrical symmetry around the z-axis:

$$\frac{1}{2}D_{zz}^{LM} = -D_{xx}^{LM} = -D_{yy}^{LM} = D_{LM}, \tag{3}$$

where the scalar quantity D_{LM} is customarily used as the coefficient of the spin–spin interaction. This equality also holds for symmetric-tops once all the equivalent interactions involving off-axis nuclei are summed over. By expressing $\mathbf{D}$ as a rank-2 spherical tensor, it is readily seen that, for a prolate top, D_{zz} accounts for the K-diagonal contribution of the spin–spin interaction *via* the tensor component $T_{2,0}(\mathbf{D})$ (see *e.g.*, eqn. (8.442) of ref. 20). In the symmetric-top basis, its matrix elements of interest ($J' = J$) are

$$\begin{aligned}&\langle J, K', \ldots | T_{2,0}(\mathbf{D}) | J, K, \ldots \rangle \\ &= -\sqrt{6} D_{LM} (-1)^{J-K'} \begin{pmatrix} J & 2 & J \\ -K' & 0 & K \end{pmatrix} \\ &\times \langle J, I_L, F_1', I_M, \ldots \| T_2(D) \| J, I_L, F_1, I_M, \ldots \rangle,\end{aligned} \tag{4}$$

and, due to the symmetry properties of the 3j-symbol, only the terms implying $K = K'$ ($\Delta K = 0$) are non-vanishing. Nonetheless, as demonstrated in some NH_3 pivotal studies,[21,22] off-diagonal matrix elements with $\Delta K = \pm 2$ can arise in some cases and, when connecting states with the same rotational energy, may become important.[23] Such energy contributions are generated by the $T_{2,\pm2}(\mathbf{D})$ tensor components, whose definition in the Cartesian axis system is

$$\begin{aligned}T_{2,\pm2}(\mathbf{D}) = -\frac{g_L g_M \mu_N^2}{4\pi\varepsilon_0 c^2} \frac{1}{R_{LM}^5} \Big[&(\mathbf{R}_{LM})_x^2 - (\mathbf{R}_{LM})_y^2 \\ &\pm i (\mathbf{R}_{LM})_x (\mathbf{R}_{LM})_y + (\mathbf{R}_{LM})_y (\mathbf{R}_{LM})_x \Big].\end{aligned} \tag{5}$$

Analogous to eqn (4), for the matrix elements of $T_{2,\pm2}(\mathbf{D})$, one has

$$\begin{aligned}&\langle J, K', \ldots | T_{2,2}(\mathbf{D}) + T_{2,-2}(\mathbf{D}) | J, K, \ldots \rangle \\ &= -D_{LM}' (-1)^{J-K'} \left[\begin{pmatrix} J & 2 & J \\ -K' & 2 & K \end{pmatrix} + \begin{pmatrix} J & 2 & J \\ -K' & -2 & K \end{pmatrix} \right] \\ &\times \langle J, I_L, F_1', I_M, \ldots \| T_2(\mathbf{D}) \| J, I_L, F_1, I_M, \ldots. \rangle\end{aligned} \tag{6}$$

This term has a non-negligible importance for $K = \pm 1$ only, *i.e.* when it connects two rotationally degenerate states. As discussed by Kukolich[23] for NH_3, this contribution is non-zero for the N–H interaction only, and it is particularly important for $^{15}NH_3$, since the ^{15}N nucleus has no quadrupole moment and terms off-diagonal in F_1 may be as large as the diagonal terms.

From an experimental point of view, the geometry that determines dipolar spin–spin coupling effects is that of the molecule at the moment of the measurements, which is usually that the molecule assumes in the vibrational ground state. Hence, in analogy to what is performed for rotational constants within the SE approach, dipolar spin–spin coupling constants should be corrected for zero-point vibrational (ZPV) effects:

$$\mathbf{D}_e^{LM} = \mathbf{D}_0^{LM} - \Delta\mathbf{D}_{ZPV}^{LM}, \tag{7}$$

where the vibrational correction, $\Delta\mathbf{D}_{ZPV}$, can be computed as implemented in CFOUR.[24] The procedure consists of expanding the expectation value over the vibrational wavefunction in a Taylor series around the equilibrium value with respect to normal-coordinate displacements, with the expansion being then truncated after the quadratic term. In the retained terms, the expectation values over normal coordinates are evaluated using perturbation theory. From a computational point of view, this procedure requires harmonic and cubic force constants being evaluated within a normal-coordinate representation. This approach has already been successfully employed for the calculation of vibrational effects on dipolar spin–spin coupling constants and other rotational parameters (see, for example, ref. 5, 25–28).

3 Methodology

As briefly mentioned in the Introduction, to demonstrate the use of the dipolar spin–spin coupling constants in structural determination, we have chosen three model systems: NH_3, PH_3, and H_2O. The hyperfine structures of these species have been extensively studied in the past and various experimental determinations of dipolar spin–spin coupling constants are present in the literature. Furthermore, their molecular geometry is completely determined by two parameters (one bond length and one angle) and, in the parent species, only two independent rotational constants are available for the structure determination. All these species possess a fluorinated counterpart, namely NF_3, PF_3, and OF_2, for which access to isotopologue data is limited, if not impossible (*i.e.* PF_3). These molecules thus provide an ideal benchmark to assess how the additional information provided by the dipolar spin–spin coupling can assist the structure determination by breaking the correlations among determinable parameters and by estimating more statistically sound uncertainties for the retrieved geometry parameters.

As a starting point of our analysis, we determined a SE equilibrium structure for each of the model molecules using a set of isotopologues: 8 for NH_3, 4 for PH_3 and 6 for H_2O. Following the standard procedure, ground state rotational constants X_0 (where $X = A$, B, and C) taken from experimental studies were computationally corrected for ZPV contributions (see Section 3.1) to obtain SE equilibrium rotational constants:

$$X_e^{SE} = X_0 + \sum_r \frac{d_r}{2} \alpha_r^X, \tag{8}$$

where d_r represents the degeneracy of the normal mode r and α_r^X is the corresponding vibration–rotation interaction constant for the X parameter. The structural parameters have then been obtained by a least-squares fit over the set of the X_e^{SE} constants, considering only the B, C pair for the planar H_2O species. Such a procedure provided the reference SE structure which the subsequent determinations are compared to. Since we do not aim at computing the "best" equilibrium structure possible for each molecule, the level of theory employed to compute the ZPV contributions has not been pushed to the limit. Furthermore, the electronic contributions to the rotational constants, ΔX_{el}, which are usually of minor importance,[33,34] have been neglected for simplicity. However, this missing contribution is taken into account when estimating the expected uncertainties of X_e^{SE} used in the data weighting scheme. Given that the fractional precision of the experimental ground state rotational constants obtained by rotational or high-resolution infrared spectroscopy is very high (10^{-8}–10^{-9}), the two main sources of uncertainties for X_e^{SE} are those due to the error on the *ab initio* computed ZPV contributions (ΔX_{ZPV}) and the lack of the electronic term ΔX_{el}.

Based on a series of previous case studies (see *e.g.* ref. 5), we assume an error of about 1% for the ZPV contributions. The corresponding relative error on the SE equilibrium rotational constants is then summed in quadrature with the fractional uncertainty due to the neglected ΔX_{el}

$$\left(\delta X_e^{SE}\right)^2 = \left(\frac{0.01\Delta X_{ZPV}}{X_e^{SE}}\right)^2 + \left(\frac{\Delta X_{el}}{X_e^{SE}}\right)^2, \qquad (9)$$

where ΔX_{ZPV} is the total ZPV contribution to a given rotational constant.

The second step is to insert the equilibrium values of the dipolar spin–spin **D** tensor elements into the structural least-squares fit. The experimental values are available for 4 isotopic species of NH_3, 6 isotopic species of H_2O and for the parent species of PH_3, NF_3, and OF_2 (see Tables 1–3). The experimental dipolar spin–spin coupling constants are corrected for the corresponding ZPV contributions using eqn (7) and then incorporated in the analysis with a weight derived from their corresponding 1σ experimental error. Given the small effect produced in the hyperfine structures by these constants, they are usually determined with a moderate precision, even when obtained by very high-resolution molecular beam measurements (*i.e.* 1% at best). Such an uncertainty is clearly dominant over the inherent inaccuracy of the *ab initio* ZPV contributions $\mathbf{\Delta D}_{ZPV}$.

Lastly, we computed a set of SE equilibrium structures using a mixed rotational/spin–spin data set from a single isotopologue for each species considered. The goodness of this last approach is evaluated in comparison with the corresponding reference structure.

3.1 Quantum chemical calculations

To have highly accurate reference values for the equilibrium dipolar spin–spin coupling constants, the equilibrium structures of the selected molecules have been obtained at the CCSD(T)/cc-pwCVQZ level of theory, with all electrons (ae) correlated but the 1s for third-row atoms. In the acronym above, CCSD(T) stands for coupled-cluster (CC) singles and doubles with perturbative treatment of triples,[42] and cc-pwCVQZ[43] is a weighted core-valence quadruple-zeta set, purposely set up for accurately describing core–core and core–valence correlation effects. For small molecules containing first- to third-row atoms,

Table 1 Spin–spin dipolar coupling constants (kHz) for ammonia isotopologues

Parameter	Experiment	*ab initio* equilibrium[a]	*ab initio* vib. averaged[a]
NH_3			
D_{NH}	4.807(35)[b]	4.738	4.594
D'_{NH}	−20.88(39)[b]	−21.538	−20.622
D_{HH}	27.524(97)[b]	28.304	27.763
$^{15}NH_3$			
D_{NH}	−6.02(25)[b]	−6.646	−6.447
D'_{NH}	31.1(19)[b]	30.214	28.934
D_{HH}	28.09(19)[b]	28.305	27.761
ND_3			
D_{ND}	0.67(16)[c]	0.728	0.710
D'_{ND}	−3.28(74)[d]	−3.306	−3.200
D_{DD}	0.56(36)[c]	0.667	0.658
$^{15}ND_3$			
D_{ND}	—	−1.020	−0.996
D'_{ND}	6.2(20)[d]	4.637	4.491
D_{DD}	—	0.667	0.658
NH_2D			
D_{yy}^{ND}	—	−2.378	−2.315
D_{xx-zz}^{ND}	—	0.201	0.190
ND_2H			
D_{yy}^{ND}	—	−1.190	−1.159
D_{xx-zz}^{ND}	—	−0.808	−0.791

[a] Computed at the ae-CCSD(T)/cc-pwCVQZ level of theory. [b] From our analysis of the molecular beam data of ref. 23, 29 and 30. [c] From ref. 31 [d] From ref. 32.

Table 2 Spin–spin dipolar coupling constants (kHz) for NF_3, PH_3, and PF_3

Parameter	Experimental	*ab initio* equilibrium[a]	*ab initio* vib. averaged[b]
NF_3			
D_{NF}	—	1.327	1.306
D'_{NF}	—	3.870	3.815
D_{FF}	11.3(67)[c]	11.133	11.014
PH_3			
D_{PH}	2.04(42)[d]	2.107	1.972
D'_{PH}	—	18.372	17.730
D_{HH}	12.65(95)[d]	13.831	13.690
PF_3			
D_{PF}	—	3.198	3.204
D'_{PF}	—	13.635	13.525
D_{FF}	—	8.199	7.891

[a] Computed at the ae-CCSD(T)/cc-pwCVQZ level of theory. [b] Zero-point vibrational contributions computed at the fc-MP2/jun-cc-pVTZ level of theory. [c] From ref. 35. [d] From ref. 36.

Table 3 Spin–spin dipolar coupling constants (kHz) for H_2O and OF_2

Parameter	Experimental	*ab initio* equilibrium[a]	*ab initio* vib. averaged[a]
H_2O			
D_{zz}^{HH}	−67.5(15)[b]	−69.668	−68.658
HDO			
D_{zz}^{HD}	−8.33(87)[c]	−8.574	−8.416
D_2O			
D_{zz}^{DD}	−1.57(41)[d]	−1.641	−1.625
$H_2{}^{17}O$			
D_{zz}^{OH}	15.67(22)[e]	16.142	15.656
$D_{xx}^{OH}-D_{yy}^{OH}$	20.53(35)[e]	21.019	20.578
D_{zz}^{HH}	−67.1(16)[e]	−69.668	−68.658
$HD^{17}O$			
D_{zz}^{OD}	5.47(62)[f]	5.030	4.919
D_{zz}^{OH}	−5.2(11)[f]	−4.188	−3.844
D_{zz}^{HD}	−8.5(19)[f]	−8.525	−8.368
$D_2{}^{17}O$			
D_{zz}^{OD}	1.64(87)[f]	2.478	2.421
D_{zz}^{DD}	—	−1.641	−1.625
OF_2			
D_{zz}^{FF}	−20.0(11)[g]	−20.042	−19.828

[a] Computed at the (CCSD(T)/cc-pwCVQZ level of theory for H_2O). For F_2O, the equilibrium values are computed at CCSD(T)/cc-pwCVQZ and zero-point vibrational contributions computed at the fc-MP2/jun-cc-VTZ level of theory. [b] From ref. 37. [c] From ref. 26. [d] From ref. 38. [e] From ref. 39. [f] From ref. 40. [g] Derived from the $\langle r^{-3}\rangle$ value reported in ref. 41.

this level of theory provides equilibrium bond lengths and angles accurate to 0.001 Å and 0.2 degrees, respectively.[34]

ZPV corrections have been computed for both rotational and dipolar spin–spin coupling constants. For the three hydrides used as model systems, the same level of the geometry optimization, *i.e.* ae-CCSD(T)/cc-pwCVQZ, has been employed. For fluorine-bearing species, to reduce the computational cost, calculations were carried out using second-order Møller–Plesset Perturbation theory (MP2),[44] within the frozen core (fc-) approximation, in conjunction with a partially augmented basis set of triple-zeta quality, *i.e.* jun-cc-pVTZ.[45,46] For phosphorous, the corresponding *d*-augmented basis set, jun-cc-pV(T+d)Z, has been employed.[46,47] Regardless of this, the basis is denoted as jun-cc-pVTZ for all the molecules considered in this work.

The computed values of the equilibrium and vibrationally averaged dipolar spin–spin coupling constants for ammonia isotopologues are reported in Table 1, and those for the other symmetric-top species NF_3, PH_3 and PF_3 are listed in Table 2. The values obtained for H_2O and OF_2 are presented in Table 3. All computations have been performed using the CFOUR package.[24,48]

4 Results and discussion

4.1 Ammonia (NH_3)

Six isotopic species have been considered for NH_3 structural determination. For each SE parameter, an average fractional uncertainty of 3×10^{-4} has been considered, which has been obtained through eqn (9) by considering average values of 3 GHz for the ZPV contribution and 75 MHz for the electronic effects.[33] This average fractional uncertainty has been used to determine the weights adopted in the fitting procedure. The structural parameters derived from 20 SE equilibrium rotational constants are listed in the first row of Table 4 and are labeled as "reference". Within the quoted error ranges (3σ for the present calculation), they are consistent with the most recent SE results from the literature[11] (also reported in Table 4), with discrepancies of 0.0003 Å for r_e(NH) and 0.11 deg. for θ_e(HNH).

Table 4 SE equilibrium structural parameters of NH_3 derived using different isotopic data sets

Data set	Iso[a] (data)	r_e(NH)/Å	θ_e(HNH)/deg.	$\sigma_{w,ROT}$[b]	$\sigma_{w,SS}$[c]
Reference	8(20)	1.0107(4)	106.83(9)	4.1	—
Mixed	8(30)	1.0106(4)	106.8338(16)	4.1	1.5
NH_3	1(5)	1.0104(4)	106.88(6)	0.3	1.1
$^{15}NH_3$	1(5)	1.0104(8)	106.87(13)	0.2	2.3
ND_3	1(4)	1.0110(4)	106.98(2)	0.0	0.3
$^{15}ND_3$	1(4)	1.0110(4)	106.98(4)	0.0	0.8
Literature[d]		1.0110(2)	106.94(2)		

Note: numbers in parentheses indicate 3σ uncertainties in units of the last quoted digit. [a] Number of isotopologues and, in parentheses, number of data. [b] Weighted rms deviation of the rotational constants. [c] Weighted rms deviation of the dipolar spin–spin coupling constants. [d] Ref. 11.

For the four top-symmetric ammonia isotopologues (NH_3, $^{15}NH_3$, ND_3 and $^{15}ND_3$), the dipolar spin–spin interaction constants were experimentally determined. In this work, values for NH_3 and $^{15}NH_3$ have been newly derived by re-analyzing the molecular beam hyperfine data for several rotation–inversion transitions available in the literature.[23,29,30] For ND_3 and $^{15}ND_3$, the spin–spin coupling parameters have been directly taken from the corresponding literature studies.[31,32] In total, 10 D_{LM} constants have been corrected for the ZPV contribution through eqn (7) and fitted together with the 20 SE equilibrium rotational constants. This new geometry is labelled as "mixed" and the corresponding parameters are reported in the second row of Table 4. It can be noticed that the inclusion of the dipolar spin–spin information has a beneficial effect in alleviating the correlation between the two geometry parameters of ammonia without producing any significant structural distortion. Indeed, the quality of the two fits is essentially the same, but the statistical uncertainty of the θ_e(HNH) is reduced by a factor of $\sim$60.

Single-isotopologue data sets, containing both rotational and SE dipolar spin–spin constants, have then been analyzed separately for each top-symmetric variant of ammonia; the derived structural parameters are presented in Table 4. The values of the structural parameters are mainly determined by the rotational constants, which are almost exactly reproduced in all cases. Still, the independent and uncorrelated information provided by the dipolar spin–spin constants (3 for NH_3 and $^{15}NH_3$ and 2 for ND_3 and $^{15}ND_3$) prevents a major distortion of the retrieved geometry and provides a meaningful estimate of the uncertainty interval. Indeed, all obtained r_e(NH) and θ_e(HNH) agree well within the statistical uncertainties.

4.2 Phosphine (PH_3)

Four isotopic variants of phosphine have been considered in the "reference": PH_3, PD_3, PH_2D, and PHD_2. An average fractional uncertainty of 1×10^{-4} has been used to estimate the weights of their SE equilibrium rotational constants. This corresponds essentially to 1% of the theoretical ZPV contributions, as the ΔX_{el} is very small ($\sim 1 \times 10^{-5}$).[49] Studies of the hyperfine spectra of PH_3 are scarcer than those of NH_3 and only two experimental determinations of dipolar spin–spin coupling constants actually exist, namely D_{PH} and D_{HH} for the parent isotopologue.[36] These two values were corrected for the ZPV contribution and used in the "mixed" structural fit. Inspection of Table 5 points out that the "reference" and "mixed" structures are essentially identical and very close to the best SE structure presently available in the literature,[49] with minor discrepancies of 7×10^{-5} Å and 0.003 deg. for r_e(PH) and θ_e(HPH), respectively. Use of the parent species only (which implies two rotational constants and two spin–spin constants as input data) does not change significantly the picture, as the derived structural parameters remain consistent within the uncertainties. Only a minor increase of the statistical error is produced, in spite of the much less parameters employed, *i.e.* 4 *vs.* 14 employed in the "mixed" structure.

4.3 Water (H_2O)

The data set for the "reference" structure of the water molecule comprises seven isotopic species: $H_2{}^{17}O$, $H_2{}^{17}O$ and their singly and doubly deuterated variants plus $H_2{}^{18}O$. Given the planarity of the molecule, only two out of three equilibrium rotational constants are actually independent and can be used simultaneously in a structural least-squares fit.[8] In the present case, the B_0, C_0 pair has been adopted. Their SE equilibrium values have been obtained, as already described for NH_3 and PH_3, by subtracting the ZPV (ae-CCSD(T)/cc-pwCVQZ) contributions from the experimental B_0, C_0. The SE equilibrium parameter weights have been estimated assuming the fractional uncertainty of 33×10^{-4}, which is obtained from eqn (9) when using average values of 5 GHz for the ZPV contribution and 150 MHz for the electronic effects.[33] The derived "reference" structural parameters are reported in the first row of Table 6.

A number of detailed studies devoted to the hyperfine structure of water rotational transitions are present in the literature. As a consequence, dipolar spin–spin coupling constants are available for six isotopologues. They are presented in Table 3 along with the corresponding literature references. The correction for the ZPV contribution through eqn (7) allowed us to obtain the set of SE equilibrium dipolar spin–spin tensor elements to be employed in the "mixed" structural calculation. For water, the "reference" and "mixed" equilibrium structures are identical, thus indicating that the structural information brought by the dipolar spin–spin coupling constants perfectly matches that established by the rotational parameters. The comparison with the most up to date SE equilibrium structure available in the literature[11] reveals small, but significant discrepancies, with r_e(OH) longer by 0.0007 Å and θ_e(HOH) smaller by 0.14 deg., both slightly exceeding the overlap range of the corresponding quoted uncertainties. This is likely due to the different treatment of the electronic contribution to the rotational constants, which may have a magnified effect on the estimate of geometrical parameters due to the planarity relationship.

Six single-isotopologue "mixed" structure calculations have been finally performed to evaluate the spread of the geometry parameters determined using the supporting contribution of the dipolar spin–spin coupling constants. Although determined with different precision, the six pairs of structural parameters make up a consistent (within 3σ) data set symmetrically spread around the "reference" geometry. This proves that the additional geometric information carried by the SE **D** tensor elements is capable of providing a reliable estimate of the distortion effects typically produced by the H–D isotopic substitution.

Table 5 SE equilibrium structural parameters of PH_3 derived using different isotopic data sets

Data set	Iso[a] (data)	r_e(PH)/Å	θ_e(HPH)/deg.	$\sigma_{w,ROT}$[b]	$\sigma_{w,SS}$[c]
Reference	4(10)	1.41188(4)	93.380(4)	0.5	—
All mixed	4(14)	1.41188(5)	93.380(4)	0.5	0.8
PH_3	1(4)	1.41193(13)	93.379(11)	0.0	0.8
Literature[d]		1.41195(8)	93.383(10)		

Note: numbers in parentheses indicate 3σ uncertainties in units of the last quoted digit. [a] Number of isotopologues and, in parentheses, number of data. [b] Weighted rms deviation of the rotational constants. [c] Weighted rms deviation of the dipolar spin–spin coupling constants. [d] Ref. 49.

Table 6 SE equilibrium structural parameters of H_2O derived using different isotopic data sets

Data set	Iso[a] (data)	r_e(OH)/Å	θ_e(HOH)/deg.	$\sigma_{w,ROT}$[b]	$\sigma_{w,SS}$[c]
Reference	7(14)	0.95798(19)	104.39(5)	1.1	—
Mixed	7(24)	0.95798(17)	104.39(5)	1.1	0.7
H_2O	1(3)	0.9581(3)	104.36(6)	0.0	0.5
HDO	1(3)	0.95832(5)	104.238(17)	0.0	0.1
D_2O	1(3)	0.95795(5)	104.422(12)	0.0	0.1
$H_2{}^{17}O$	1(5)	0.9581(2)	104.36(5)	0.0	0.4
$HD^{17}O$	1(5)	0.9578(6)	104.42(18)	0.1	1.0
$D_2{}^{17}O$	1(3)	0.9577(5)	104.48(11)	0.0	1.0
Literature[d]		0.9573(1)	104.53(1)		

Note: numbers in parentheses indicate 3σ uncertainties in units of the last quoted digit. [a] Number of isotopologues and, in parentheses, number of data. [b] Weighted rms deviation of the rotational constants. [c] Weighted rms deviation of the dipolar spin–spin coupling constants. [d] Ref. 11.

4.4 Fluorinated species (NF_3, OF_2, and PF_3)

Minimal data sets are available for the fluorinated analogues of the chosen model molecules. For NF_3, the experimental values of the B_0 and C_0 constants were determined, while only B_0 is available for $^{15}NF_3$.[53,54] The experimental value of the dipolar spin–spin D_{FF} constant for the main isotopic species has been reported by Novick *et al.*[35] The B_0 and C_0 constants of PF_3 have been determined in several infrared investigations; here, we use the value provided by Najib (2014).[51] Instead, no experimental information on its hyperfine structure is presently available in the literature. To the best of our knowledge, only the rotational

spectrum of the parent species of OF_2 has been investigated and its ground state rotational constants still come from a microwave study performed in the 60's.[55] An estimate of the F–F dipolar spin–spin coupling constants was obtained by molecular beam electric resonance measurements more than twenty years later.[41]

The SE equilibrium values for the rotational and spin–spin coupling constants of these three species have been obtained using the ZPV contributions computed in this work (fc-MP2/jun-cc-pVTZ) and then employed to derive the "mixed" equilibrium structures. As performed for the model molecules in previous sections, the weights of the rotational constants have been set to 1×10^{-4} of the corresponding values, mostly on the basis of the ZPV contribution accuracy. The impact of the electronic contributions has been estimated from the g constants[56,57] and was found to be essentially negligible. The derived structural parameters are reported in Table 7 together with the best available equilibrium geometries from the literature.[50–52]

For NF_3 and OF_2, our "mixed" SE approach yields equilibrium geometrical parameters more precise than those available in the literature, with the set two sets of values agreeing within the quoted error ranges. The only exception is the O–F bond length in OF_2 for which our determination provides a value 0.001 Å longer than the corresponding literature value. However, it should be noted that the values of r_e(XF) and θ_e(FXF) from ref. 50–52 were obtained using a minimal set of constants and, being purely experimental, they may also be affected by residual perturbations on the retrieved equilibrium rotational constants. This aspect is particularly critical for PF_3, for which the two structural parameters were derived from only two rotational constants and the uncertainty range, estimated by error propagation, is clearly underestimated (Table 7). Unfortunately, the lack of any experimental information on the dipolar spin–spin coupling prevents us from computing a "mixed" equilibrium structure for PF_3 and providing a reliable uncertainty range on its geometry parameters. In Table 7, the structural parameters optimized at the ae-CCSD(T)/cc-pwCVQZ level of theory are also reported. Their comparison with the literature and SE results points out a good agreement. In view

Table 7 SE equilibrium structural parameters of the fluorinated species considered

Data set	Iso[a] (data)	r_e(XF)/Å	θ_e(FXF)/deg.	$\sigma_{w,ROT}$[b]	$\sigma_{w,SS}$[c]
NF_3	2(4)	1.36797(3)	101.878(3)	0.0	0.1
Literature[d]		1.3675(10)	101.86(10)		
Theory[e]		1.366	101.9		
PF_3[f]	1(2)	1.56111	97.561		
Literature[g]		1.560986(43)	97.566657(64)		
Theory[e]		1.561	97.6		
OF_2	1(3)	1.40625(18)	103.08(2)	0.0	0.3
Literature[h]		1.4053(4)	103.07(5)		
Theory[e]		1.403	103.1		

Note: Numbers in parentheses indicate 3σ uncertainties in units of the last quoted digit. [a] Number of isotopologues and, in parentheses, number of data. [b] Weighted rms deviation of the rotational constants. [c] Weighted rms deviation of the dipolar spin–spin constants. [d] Average values from ref. 50. [e] At the ae-CCSD(T)/cc-pwCVQZ level of theory. [f] No degrees of freedom, thus errors cannot estimated. [g] Experimental value from ref. 51. Uncertainties obtained by error propagation. [h] Experimental value from ref. 52.

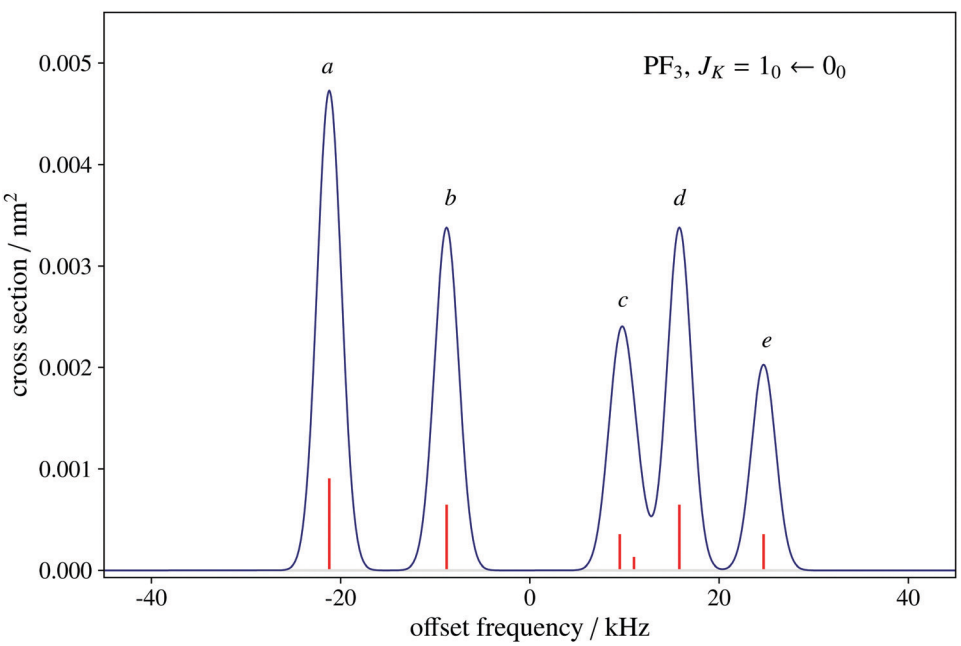

Fig. 1 Spectral simulation of the $J_K = 1_0 - 0_0$ rotational transition of PF_3 as can be observed using a pulsed-jet Ball–Flygare Fourier-transform microwave spectrometer. The x-axis scale is expressed as the offset with respect to the unperturbed frequency value of 15637.959 MHz. The y-axis scale indicates the absorption cross section computed at 2 K, the typical rotational temperature obtained in a supersonic-jet cooled sample. The hyperfine components are labelled as $F_1', F' \leftarrow F_1, F$. (*a*) 1.5,3 ← 0.5,2; (*b*) 1.5,2 ← 0.5,1 and 1.5,2 ← 0.5,2; (*c*) 1.5,1 ← 0.5,1, 1.5,1 ← 0.5,2, and 1.5,0 ← 0.5,1; (*d*) 1.5,2 ← 0.5,1 and 1.5,2 ← 0.5,2; (*e*) 1.5,1 ← 0.5,1 and 1.5,1 ← 0.5,2. The I_{tot} for $K = 0$ is always 1.5 because of spin statistics.

of the accuracy of ae-CCSD(T)/cc-pwCVQZ geometries discussed above,[34] the observed agreement supports the reliability of the SE/experimental structural determinations even when carried out with a very limited number of data.

To date, there are no studies devoted to the hyperfine structure of the rotational transitions of PF_3, despite the fact that the $J = 1 \leftarrow 0$ line is located at 15.6 GHz, a frequency region easily achievable using a Ball–Flygare-type high-resolution Fourier-transform microwave (FT-MW) spectrometer (see *e.g.* ref. 58). Our theoretical calculations provide a full characterization of the hyperfine structure of this transition and provide a valuable guide for future laboratory measurements. Besides the P–F and F–F dipolar spin–spin coupling constants listed in Table 2, we have also computed the nuclear spin-rotation coupling tensor **C** for the P and F nuclei at the ae-CCSD(T)/cc-pwCVQZ level of theory. The values of the isotropic constant ($C_{iso} = \frac{1}{3}\mathrm{Tr}(\mathbf{C})$) are $C_{iso}(F) = -12.77$ kHz and $C_{iso}(P) = -9.23$ kHz. The hyperfine pattern of the $J = 1 \leftarrow 0$ rotational transition of PF_3 has then been evaluated using the SPCAT program[59] and is plotted in Fig. 1 assuming a typical pulsed-jet FT-MW line full width at half maximum of 3 kHz. Under these experimental conditions, the hyperfine structure of the $J = 1 \leftarrow 0$ transition is predicted to be well resolved. This indicates that its spectral analysis would lead to an accurate determination of dipolar spin–spin coupling constants, thus opening the route towards a complete structural determination of PF_3.

5 Conclusions

In this perspective, we have investigated the use of dipolar spin–spin coupling constants in the structure determination of isolated molecules. The SE approach is powerful and allows the determination of equilibrium geometries with minimum experimental efforts. However, it is effective only if the number of available isotopic substitutions is greater than the number of internal coordinates describing the molecular system. Furthermore, an unbalanced set of data due to impossible isotopic substitution (as in the case of F and P) can lead to biased results. In those cases for which obtaining a sufficiently large set of data is unpractical due to the lack of isotopic data or totally unfeasible (as for PF_3), dipolar spin–spin coupling constants can be considered as an additional source of information for the SE least-squares fitting procedure. Spin–spin coupling in rotational spectra only produces small effects, usually detected as perturbations of more important interactions, such as nuclear quadrupole coupling and/or nuclear spin-rotation interactions. In the past, the determination of dipolar spin–spin constants was a prerogative of molecular beam maser techniques, which are characterized by an extremely high resolving power. Nowadays, adequate resolution to reveal spin–spin coupling effects is achievable routinely using a Fourier-transform spectrometer coupled with supersonic expansions of the gas sample. Although experimentally determined with moderate precision (typically 1–10%), the dipolar spin–spin coupling constants can effectively support the determination of the molecule structural parameters within the SE approach. Their incorporation in an isotopically balanced fit does not generally alter the value of the structural parameters, but can lead to a significant reduction of their statistical error, as they provide independent and statistically uncorrelated information for the least-squares fit procedure. In critical cases, when there is a shortage of isotopic rotational data, their inclusion in the computation provides additional degrees of freedom (thus leading to a significant improvement of the fit and geometrical parameters).

Conflicts of interest

There are no conflicts to declare.

Acknowledgements

This work was supported by the MIUR (PRIN Grant Number 202082CE3T) and the University of Bologna (RFO funds). The SMART@SNS Laboratory (**http://smart.sns.it**) is acknowledged for providing high-performance computing facilities.

Notes and references

1 *Accurate molecular structures: their determination and importance*, ed. A. Domenicano and I. Hargittai, Oxford University Press, Oxford, UK, 1992.
2 *Equilibrium Molecular Structures: From Spectroscopy to Quantum Chemistry*, ed. J. Demaison, J. E. Boggs and A. G. Császár, CRC Press, Taylor & Francis Group, Boca Raton, FL, US, 2011.
3 A. Mazzanti and D. Casarini, *WIREs Comput. Mol. Sci.*, 2012, **2**, 613–641.
4 *Computational Strategies for Spectroscopy, from Small Molecules to Nano Systems*, ed. V. Barone, John Wiley & Sons, Inc., Hoboken, New Jersey, 2011.
5 C. Puzzarini, J. F. Stanton and J. Gauss, *Int. Rev. Phys. Chem.*, 2010, **29**, 273–367.
6 C. Puzzarini, J. Bloino, N. Tasinato and V. Barone, *Chem. Rev.*, 2019, **119**, 8131–8191.
7 V. Barone, S. Alessandrini, M. Biczysko, J. R. Cheeseman, D. C. Clary, A. B. McCoy, R. J. DiRisio, F. Neese, M. Melosso and C. Puzzarini, *Nat. Rev. Methods Primers*, 2021, **1**, 1–27.
8 W. Gordy and R. L. Cook, *Microwave molecular spectra*, Wiley, New York, 1984.
9 P. Pulay, W. Meyer and J. E. Boggs, *J. Chem. Phys.*, 1978, **68**, 5077–5085.
10 F. Pawłowski, P. Jørgensen, J. Olsen, F. Hegelund, T. Helgaker, J. Gauss, K. L. Bak and J. F. Stanton, *J. Chem. Phys.*, 2002, **116**, 6482–6496.
11 M. Piccardo, E. Penocchio, C. Puzzarini, M. Biczysko and V. Barone, *J. Phys. Chem. A*, 2015, **119**, 2058–2082.
12 C. Puzzarini and V. Barone, *Acc. Chem. Res.*, 2018, **51**, 548–556.
13 C. Degli Esposti, M. Melosso, L. Bizzocchi, F. Tamassia and L. Dore, *J. Mol. Struct.*, 2019, **1203**, 127429.

14 H. Ye, M. Mendolicchio, H. Kruse, C. Puzzarini, M. Biczysko and V. Barone, *J. Mol. Struct.*, 2020, **1211**, 127933.
15 J. Lei, S. Alessandrini, J. Chen, Y. Zheng, L. Spada, Q. Gou, C. Puzzarini and V. Barone, *Molecules*, 2020, **25**, 4899.
16 D. A. Obenchain, L. Spada, S. Alessandrini, S. Rampino, S. Herbers, N. Tasinato, M. Mendolicchio, P. Kraus, J. Gauss and C. Puzzarini, *et al.*, *Angew. Chem., Int. Ed.*, 2018, **57**, 15822–15826.
17 X. Li, L. Spada, S. Alessandrini, Y. Zheng, K. G. Lengsfeld, J.-U. Grabow, G. Feng, C. Puzzarini and V. Barone, *Angew. Chem., Int. Ed.*, 2022, **61**, e202113737.
18 J. Kraitchman, *Am. J. Phys.*, 1953, **21**, 17–24.
19 A. Abragam, *The principles of nuclear magnetism*, Clarendon Press, Oxford, 1989.
20 J. M. Brown and A. Carrington, *Rotational Spectroscopy of Diatomic Molecules*, Cambridge University Press, 2003.
21 G. R. Gunther-Mohr, C. H. Townes and J. H. van Vleck, *Phys. Rev.*, 1954, **94**, 1191–1203.
22 J. P. Gordon, *Phys. Rev.*, 1955, **99**, 1253–1263.
23 S. G. Kukolich, *Phys. Rev.*, 1967, **156**, 83–92.
24 J. F. Stanton, J. Gauss, L. Cheng, M. E. Harding, D. A. Matthews and P. G. Szalay, CFOUR, Coupled-Cluster techniques for Computational Chemistry, a quantum-chemical program package, with contributions from A. A. Auer, R. J. Bartlett, U. Benedikt, C. Berger, D. E. Bernholdt, Y. J. Bomble, O. Christiansen, F. Engel, R. Faber, M. Heckert, O. Heun, M. Hilgenberg, C. Huber, T.-C. Jagau, D. Jonsson, J. Jusélius, T. Kirsch, K. Klein, W. J. Lauderdale, F. Lipparini, T. Metzroth, L. A. Mück, D. P. O'Neill, D. R. Price, E. Prochnow, C. Puzzarini, K. Ruud, F. Schiffmann, W. Schwalbach, C. Simmons, S. Stopkowicz, A. Tajti, J. Vázquez, F. Wang, J. D. Watts and the integral packages MOLECULE (J. Almlöf and P. R. Taylor), PROPS (P. R. Taylor), ABACUS (T. Helgaker, H. J. Aa. Jensen, P. Jørgensen, and J. Olsen), and ECP routines by A. V. Mitin and C. van Wüllen. For the current version, see **http://www.cfour.de**.
25 C. Puzzarini, G. Cazzoli, M. E. Harding, J. Vázquez and J. Gauss, *J. Chem. Phys.*, 2009, **131**, 234304.
26 G. Cazzoli, V. Lattanzi, J. L. Alonso, J. Gauss and C. Puzzarini, *Astroph. J.*, 2015, **806**, 100.
27 M. Melosso, L. Dore, J. Gauss and C. Puzzarini, *J. Mol. Spectrosc.*, 2020, **370**, 111291.
28 M. Melosso, M. L. Diouf, L. Bizzocchi, M. E. Harding, F. M. Cozijn, C. Puzzarini and W. Ubachs, *J. Phys. Chem. A*, 2021, **125**, 7884–7890.
29 S. G. Kukolich, *Phys. Rev.*, 1968, **172**, 59–63.
30 S. G. Kukolich and S. C. Wofsy, *J. Chem. Phys.*, 1970, **52**, 5477–5481.
31 R. Garvey, F. De Lucia and J. Cederberg, *Mol. Phys.*, 1976, **31**, 265–287.
32 J. van Veldhoven, R. T. Jongma, B. Sartakov, W. A. Bongers and G. Meijer, *Phys. Rev. A: At., Mol., Opt. Phys.*, 2002, **66**, 032501.
33 C. Puzzarini, M. Heckert and J. Gauss, *J. Chem. Phys.*, 2008, **128**, 194108.
34 S. Coriani, D. Marchesan, J. Gauss, C. Hättig, T. Helgaker and P. Jørgensen, *J. Chem. Phys.*, 2005, **123**, 184107.
35 S. E. Novick, W. Chen, M. R. Munrow and K. J. Grant, *J. Mol. Spectrosc.*, 1996, **179**, 219–222.
36 G. Cazzoli and C. Puzzarini, *J. Mol. Spectrosc.*, 2006, **239**, 64–70.
37 G. Cazzoli, C. Puzzarini, M. E. Harding and J. Gauss, *Chem. Phys. Lett.*, 2009, **473**, 21–25.
38 G. Cazzoli, L. Dore, C. Puzzarini and J. Gauss, *Mol. Phys.*, 2010, **108**, 2335–2342.
39 C. Puzzarini, G. Cazzoli, M. E. Harding, J. Vázquez and J. Gauss, *J. Chem. Phys.*, 2009, **131**, 234304.
40 C. Puzzarini, G. Cazzoli, M. E. Harding, J. Vázquez and J. Gauss, *J. Chem. Phys.*, 2015, **142**, 124308.
41 R. L. DeLeon, D. Prichard and J. S. Muenter, *J. Chem. Phys.*, 1985, **83**, 4962–4966.
42 K. Raghavachari, G. W. Trucks, J. A. Pople and M. Head-Gordon, *Chem. Phys. Lett.*, 1989, **157**, 479–483.
43 K. A. Peterson and T. H. Dunning Jr., *J. Chem. Phys.*, 2002, **117**, 10548–10560.
44 C. Møller and M. S. Plesset, *Phys. Rev.*, 1934, **46**, 618.
45 T. H. Dunning Jr., *J. Chem. Phys.*, 1989, **90**, 1007.
46 E. Papajak and D. G. Truhlar, *J. Chem. Theory Comput.*, 2011, **7**, 10–18.
47 D. E. Woon and T. H. Dunning, *J. Chem. Phys.*, 1993, **98**, 1358–1371.
48 D. A. Matthews, L. Cheng, M. E. Harding, F. Lipparini, S. Stopkowicz, T.-C. Jagau, P. G. Szalay, J. Gauss and J. F. Stanton, *J. Chem. Phys.*, 2020, **152**, 214108.
49 J. Breidung and W. Thiel, *J. Phys. Chem. A*, 2019, **123**, 5600–5612.
50 J. Breidung, L. Constantin, J. Demaison, L. Margulès and W. Thiel, *Mol. Phys.*, 2003, **101**, 1113–1122.
51 H. Najib, *J. Mol. Spectrosc.*, 2014, **305**, 17–21.
52 Y. Morino and S. Saito, *J. Mol. Spectrosc.*, 1966, **19**, 435–453.
53 G. Cazzoli and C. Puzzarini, *J. Mol. Spectrosc.*, 2006, **239**, 59–63.
54 H. Najib, N. Ben Sari-Zizi, J. Demaison, B. Bakri, J. M. Colmont and E. B. MKadmi, *J. Mol. Spectrosc.*, 2003, **220**, 214–222.
55 L. Pierce, R. Jackson and N. DiCianni, *J. Chem. Phys.*, 1961, **35**, 2240–2241.
56 W. Flygare and R. Benson, *Mol. Phys.*, 1971, **20**, 225–250.
57 D. J. Wilson, C. E. Mohn and T. Helgaker, *J. Chem. Theory Comput.*, 2005, **1**, 877–888.
58 L. Bizzocchi, B. M. Giuliano and J.-U. Grabow, *J. Mol. Struct.*, 2007, **833**, 175–183.
59 H. M. Pickett, *J. Mol. Spectrosc.*, 1991, **148**, 371–377.